

## Computational Fluid Dynamics Study of Blood Flow in Aorta using OpenFOAM

Open  
Access

Mohamad Shukri Zakaria<sup>1,2,\*</sup>, Farzad Ismail<sup>3</sup>, Masaaki Tamagawa<sup>4</sup>, Ahmad Fazli Abdul Azi<sup>6</sup>, Surjatin Wiriadidjaya<sup>1</sup>, Adi Azrif Basri<sup>1</sup>, Kamarul Arifin Ahmad<sup>1,5</sup>

<sup>1</sup> Department of Aerospace Engineering, Faculty of Engineering, Universiti Putra Malaysia, 43400 Serdang, Selangor, Malaysia

<sup>2</sup> Faculty of Mechanical Engineering, Universiti Teknikal Malaysia Melaka, Hang Tuah Jaya 76100, Durian Tunggal, Melaka, Malaysia

<sup>3</sup> School of Aerospace Engineering, Universiti Sains Malaysia, Nibong Tebal, Pulau Pinang, 14300, Malaysia

<sup>4</sup> Graduate School of Life Science and Systems Engineering, Kyushu Institute of Technology, Kitakyushu 808-0916, Japan

<sup>5</sup> Mechanical Engineering Department, College of Engineering, King Saud University, P.O. Box 800, Riyadh 11421, Saudi Arabia

<sup>6</sup> Cardiology Specialist Clinic, Hospital Serdang, 43400 Serdang, Selangor, Malaysia

### ARTICLE INFO

#### Article history:

Received 5 January 2018

Received in revised form 19 February 2018

Accepted 2 March 2018

Available online 10 March 2018

### ABSTRACT

Understanding of flow pattern behaviour inside the aorta contributes significantly in diseases treatment artificial design. Objective of present study is to simulate the blood flow in patient specific aorta using open source computational fluid dynamics (CFD) platform OpenFOAM. The real geometry was obtained from real male Malaysian patient. There are not much data available in literature incorporate real geometry of aorta due to complex geometry. The validation is done against existing experimental result of the 90 degree curve tube model. It was shown that our method is able to capture complex flow in the curve tube like secondary and separation flow that responsible for development of wall shear stress at the tube wall. These flow physics could have similarity in aorta blood flow. Finally, we apply our method with anatomy human aorta with pulsatile inlet condition. Further comparison is made with unstructured boundary fitted mesh. The final result shows that the detailed flow physics can be captured in an aorta.

#### Keywords:

Computational fluid dynamics,  
OpenFOAM, blood flow, aorta

Copyright © 2018 PENERBIT AKADEMIA BARU - All rights reserved

## 1. Introduction

The human aorta is a major blood vessel in our heart system, and its complexity including curvature in several planes, branches at apex of the arch, significant tapering and with distensible vessel wall. The important of Computational Fluid Dynamics (CFD) study for a blood flow is numerous, for example, it could predict thrombus potential, and also heart valve hemodynamics study [1]. CFD method has the advantage that can provide useful information such as vortices shear stress, and vertical structural that expensive and impossible to obtained using in-vitro or in-vivo study.

\* Corresponding author.

E-mail address: [mohamad.shukri@utem.edu.my](mailto:mohamad.shukri@utem.edu.my) (Mohamad Shukri Zakaria)

A common and continuous problem for CFD simulation in biomedical field is that the lack of real patient geometry, lack of validation, low resolution turbulent modelling, and inaccurate formulation for blood clot estimation. Blood clot may detach and travel to the brain causing stroke and sudden death. Existence of blood clot may result from vascular stenosis caused by atherosclerosis [2]. Atherosclerosis is a disease in which plaque builds up inside your arteries due to unhealthy lifestyle. Previous study that uses CFD in aorta blood flow can found in [3,4]. Biasseti *et al.*, [5] used the vortical structure of an education scheme  $\lambda_2$  [6], with a non-Newtonian fluid to identify areas of blood clot potential in the aorta. Naimah *et al.* [7] superimposed the vortical structure with the region where low wall shear stress ( $<0.5$  Pa) to predict blood clot location.

Similarly, Anupindi *et al.*, [8] used to visualize the long vortical structures in the aorta, but the clinical significance of these structures has yet to be understood. Furthermore turbulent large eddy simulation (LES) model with a patient-specific aorta based on the  $\lambda_2$  criterion would be the most suitable method for problems related to biological fluids, such as blood [5], compared to the Q criterion, seeded particle and multiphase flow to correlate the blood clot formation [9]. However, there are small scale vertical structure may generated due to numerical noise cause of the use of  $\lambda_2$  criterion compare to Q criterion [10]. Moreover, the used of idealized aorta was underpredict the flow structure and thus unable to accurately estimate the blood clot potential [11].

In this paper, we analysed the blood clot potential in the patient specific aorta, through LES formulation on open source software OpenFOAM. OpenFOAM was used by many field, for example in aerodynamics [12], but not well explored in biomedical field. The use of real patient specific aorta and high resolution turbulent model (i.e, large eddy simulation) and Q criterion for vertical structural visualization was also integrated in this study. It is believe that the complex flow may contribute to the increase in the residential time of the red blood cells in the relatively high turbulent shear stress region may have influencing the potential for significant platelet activation and blood clot formation.

## 2. Methodology

### 2.1 Mathematical Equation and Numerical Method

The blood is assume to be incompressible fluid with the equation of continuity, and momentum as follows

$$\nabla \cdot \mathbf{u} = 0 \quad (1)$$

$$\frac{\partial(\rho\mathbf{u})}{\partial t} + \nabla \cdot (\rho\mathbf{u}\mathbf{u}) - \nabla \cdot (\mu\nabla\mathbf{u}) - (\nabla\mathbf{u}) \cdot \nabla\mu = -\nabla p \quad (2)$$

where  $\mathbf{u}$  is velocity vector,  $p$  is pressure,  $\mu$  is viscosity and  $\rho$  is density.

Numerical scheme to discretize above equations is based on OpenFOAM solver and is extension of our work in Zakaria *et al.*, [13]. It was solved term by term basis. Finite volume method on collocated grid arrangement was used. Temporal term was treat with Euler implicit, convection term with linear scheme while diffusion term with upwind scheme Euler implicit is used.

Simple linear matrix solvers [14] have been used in all cases. Pressure and pressure correction equations are solved with a Preconditioned Conjugate Gradient solver (PCG), using diagonal incomplete-Cholesky preconditioner (DIC), while velocity, colour function and turbulence quantities are solved using smoothSolver and GaussSiedel smoother. Each outer iteration matrices are solved until an absolute residual of  $10^{-6}$  is achieved.

## 2.2 Validation

Flow through 90 degree bend pipe is essential a step forward in understanding flow characteristic on the human aorta. Such methodology is previously used in [15-17]. This is because the geometry of the ascending and descending aorta is almost similar with curve pipe [18], thus similar complex flow characteristic such as secondary flow should be observed. In this paper, we validate our numerical algorithm through flow on 90 degree bend against well-known existing experimental work done by Van de Vosse *et al.*, [19].

The results of velocity magnitude obtained are extracted at exit curved location. As seen in Fig. 1, the calculated velocity profiles are in excellent agreement with the experiment measurements in [19]. Furthermore, these plots show the considerable deformation of the velocity profile in the curved part of the pipe and the shift in the location of maximum. In Fig. 2, the velocity contour map of the axial velocity distribution in pipe cross-sections at five consecutive cross-sections in the curved part of the pipe is shown. In the top half of the plots the experimental results by Van de Vosse *et al.*, [19] are also shown, while in the bottom half our numerical results are shown. Again, qualitative comparison shows very good agreement with the experimental measurement. Therefore, we can say that our method and numerical algorithm is validated.

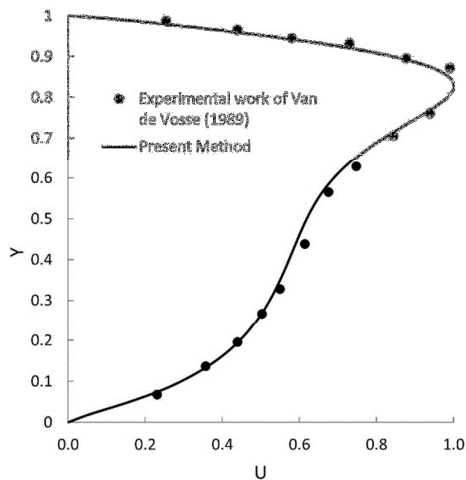


**Fig. 1.** Flow solver validation. The flow solver agrees closely with experimental results measured in the center plane of the tube at the end of the curved section

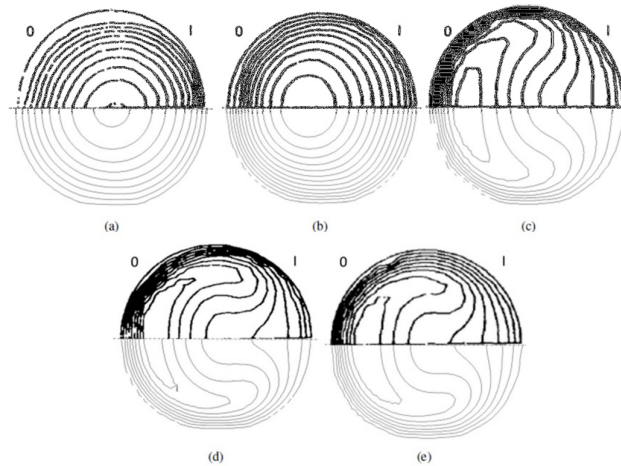


**Fig. 2.** Velocity contour maps; a) 0 degree, b) 22.5 degree, c) 45 degree, d) 67.5 degree and e) 90 degree, (I: inner curve, O: outer curve). The results presented in the upper half of the figure were derived by Van de Vosse *et al.*, [19]. Our numerical results are given in the bottom half

## 2.3 Geometry of Aorta

The CT scan was obtained from the anatomical model of a male 71 year old Malaysian subject (Fig. 3). The scans produced a total of 1023 slices of axial, coronal and sagittal images, which accounted for the complete heart area, from aorta to ventricular. The increment between each slice of the scan images is 0.7 mm and the slice thickness is 1 mm. The scan images were segmented slice by slice with an appropriate threshold value using Mimics (Materialise, Ann Arbor, MI).

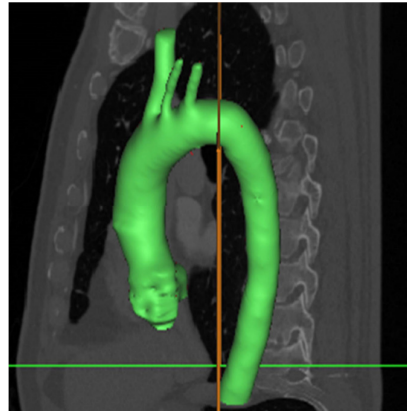


**Fig. 3.** Segmented aorta from MIMICS images of real patient data

#### 2.4 Computational Domain

Uniform block cell is generate using blockMesh utilities on whole constructed domain at first. This block cell is representing hexahedral cell that we will fully utilize for its excellent mesh quality. The mesh is then castellated using snappyHexMesh utilities in OpenFOAM.

Boundary condition is set at 1 inlet and 4 outlet of the aorta model. At the inlet, a flat spatial velocity profile was imposed, allowing the flow to develop fully naturally. This imposed velocity varied with a pulsatile waveform, based on measured beating heart condition as shown in sub-figure in Fig. 4. The effect of pulsatile flow implement in this study is following work of Biasetti *et al.*, [5] with heart rate of 70 beats/min (corresponding to an 860 ms cardiac cycle time). The uses of pulsatile inlet flow is important so that it could account for both inertial and viscous effect. The location of the inlet is virtually place on valve location. An opening boundary condition with relative static pressure of 0 Pa was specified at all 4 outlet of the aorta.

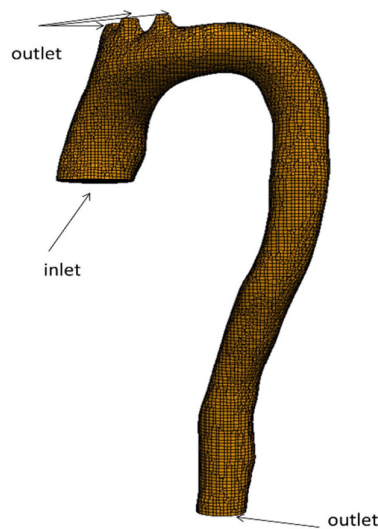


**Fig. 4.** Geometry with boundary condition and meshed structure

The arterial wall was treated as solid, rigid, non-permeable and a no-slip boundary condition was applied. Blood was assumed be a Newtonian and incompressible fluid with kinematic viscosity of  $4 \times 10^{-6} \text{ m}^2/\text{s}$  and a density of  $1050 \text{ kg/m}^3$ . Based on nominal diameter of the aorta, peak pulsatile flow could yield Reynolds number of 5000-6000. This is turbulent flow condition. The turbulent model uses in the present study is based on the available model in OpenFOAM. We choose LES  $k$ -equation eddy viscosity model (also known as oneEqEddy) in our analysis.

The grid independency test result is shown in Figure 5. The velocity profile at the ascending aorta location, Slice B (refer Figure 6) is plotted. The solver used for the boundary fitted method is based on the existing pimpleFoam solver in OpenFOAM. The solver is well validated such as by [20] and could serve as a benchmark for this study. As seen, the velocity profile for both methods converged when the grid is refined. Except that, the peak velocity is slightly different in the inner curvature of aorta (as elaborated further in the succeeding discussion). It is expected that as the total number of grid elements increases, the maximum velocity becomes closer to the finest grid.

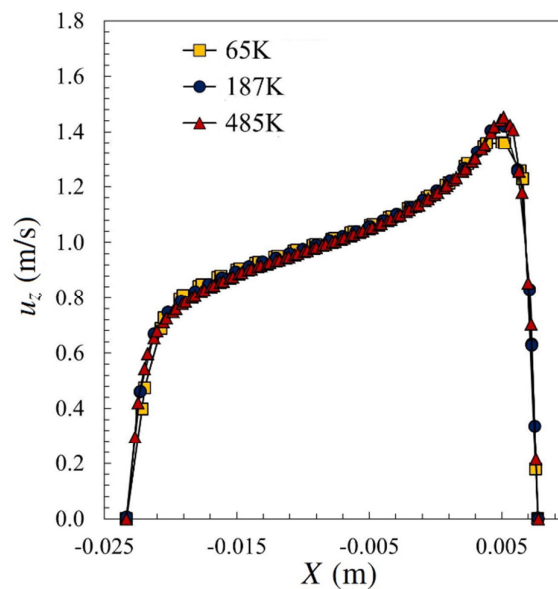
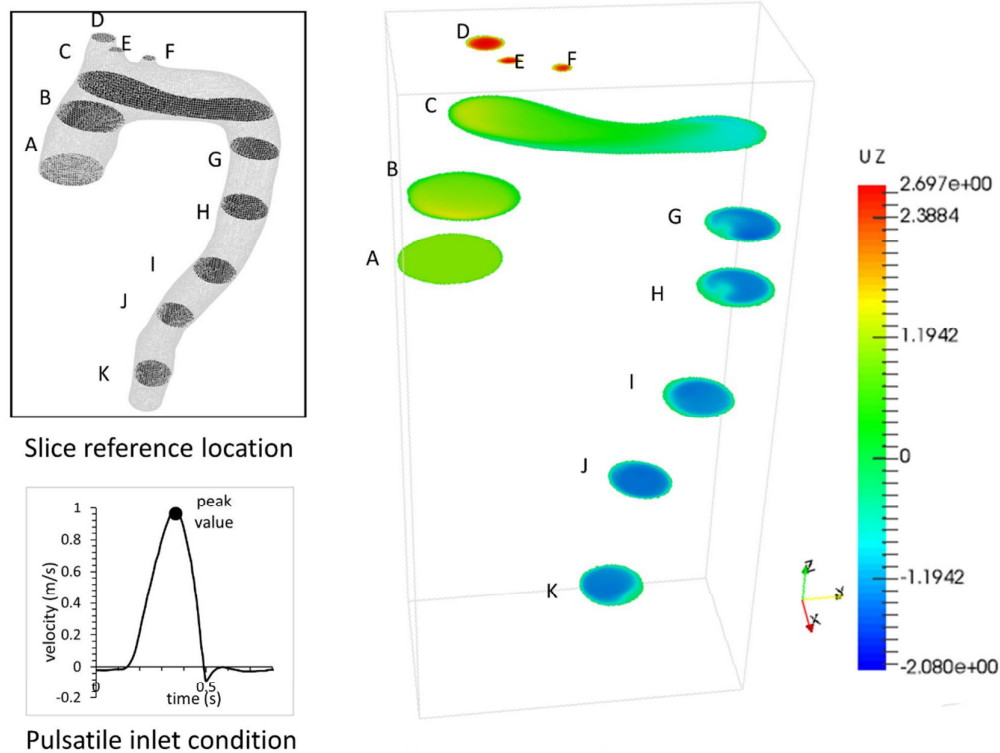


Fig. 5. Grid independent study on axial velocity at centerline of aorta at slice B (Refer Fig. 6)

### 3. Results and Discussion

Figure 6 shows a general comparison of the velocity contour. Eleven (11) slice locations were made, denoted by the uppercase letters A-K. Pulsatile inlet condition was imposed at the inlet, with the velocity contour shown at a peak velocity of 1m/s. As observed, an identical velocity contour was found for those two methods for all 11 slice locations. A complex flow helical pattern is also seen. For example, at the ascending aorta (slice A, B, C), the flow velocity is at a maximum at the outer part of the bend. At the early descending aorta (slice G, H, I), the maximum flow is located at the inner curve, but then returns back into the outer curvature at the end of the descending aorta (slice J, K). It is also clear that the complexity of the aorta geometry has a strong influence on the downstream flow.



**Fig. 6.** Velocity contour at several slice locations during the time of the peak flow. The left bottom subfigure is pulsatile flow imposed at the inlet

To examine the complex flow patterns in ascending and descending aorta in greater detail, the flow is visualized through slice B and slice G corresponding to ascending and descending aorta respectively as depicted in Fig. 7. Here, the velocity contour for the representative phases of the pulsatile cardiac cycle (early accelerate flow, peak flow and decelerate flow) are shown, corresponding to systolic and diastolic instantaneous time of 0.25s, 0.35s and 0.45s respectively. The choice of time instant is based on the fact that the valve is in fully open position, so that the effect of turbulent could be minimize since the geometry of heart valve is completely neglected in this study.

During accelerate flow at the ascending aorta, velocity is higher close to inner curve, with the secondary flow is uniformly migrate to that inner curve. A rapidly flowing fluid with a large momentum near the outer curve is forced inward along the wall and reaches the inner curve region due to the strong secondary flow occurring in the cross section behind the bend entrance. Compared to the descending aorta, a much lower overall jet velocity is observed. At the descending aorta, similar uniform secondary flow is observed, but the velocity magnitude is significantly higher near outer curve.

During peak flow, helical secondary flow vector is observed near outer and inner curve. Similar with descending aorta, the formation of vortex is prominent. This proved that our numerical simulation could provide unsteadiness and complex flow detail. These observation suggested that the secondary flow structures resulting from the aorta curvature contributed to the transverse spread of the jets by impeding their downstream motion. It is possible that secondary flow structures contribute to the reduction of turbulent and viscous stresses in other ways such as by stabilizing the shear layers between the jets.

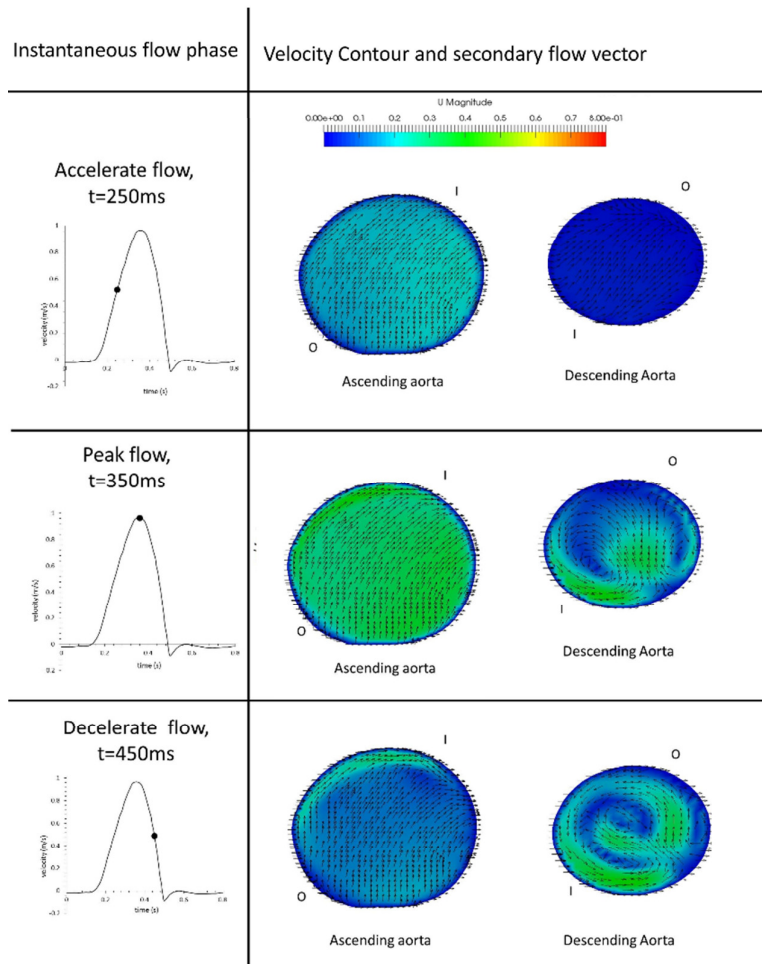


**Fig. 7.** z velocity contour at cross section B, (I: inner curve, O: outer curve)

Three-dimensional vortical structures are visualised in Figure 8 using the Q criterion [21] for at different time instants within the cardiac cycle. These vortical structures may lead to potential platelet activation and thrombosis, where the flow is entrapped in the circulation region [5,7]. The vortical structure Q is defined as  $Q=0.5 (||\Omega||^2 - ||S||^2)$ , where, S and W denote the symmetric and antisymmetric parts of the velocity gradient, respectively, and  $|| \bullet ||$  is the Euclidean matrix norm. The fundamental definition of  $Q > 0$  is refer to those where the rotation rate dominates the strain rate are occupied by vertical structures [21].

At the AF phase ( $t = 0.25$  s), small-scale chaotic vortical structures are formed. Structures are well organised and laminar but are later broken down in an explosive manner into smallscale chaotic vortical structures at the  $t = 0.35$  s and  $t = 0.45$  s. At the  $t = 0.35$  s, large vortical structures are created by the curvature-induced secondary currents in the arch. Furthermore, the arch region is composed of elongated vortical structures that originate close to the inner wall of the ascending aortic arch and extend towards the outer wall of the descending arch.

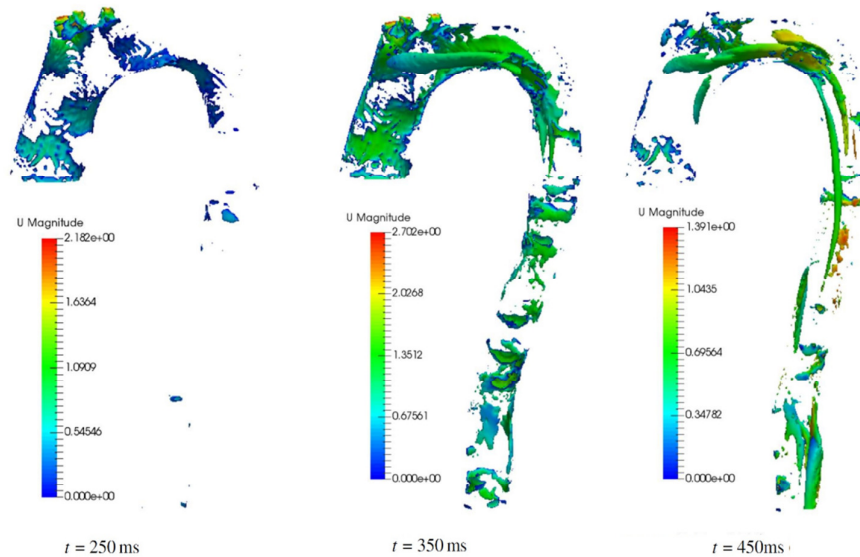


**Fig. 8.** Instantaneous vortical structure by the Q-criterion, coloured by velocity magnitude, at different instantaneous pulsation time

#### 4. Conclusion

The present study provide the usage of CFD open source platform OpenFOAM in simulating biomedical application. The transient incompressible solver, namely PimpleFOAM was previously validated in [20]. The numerical study briefly discussed above indicate the following characteristics of flow development in the aorta.

1. The axial velocity profiles at various cross-sections indicate relatively flat velocity profiles during systole with a skew towards the inner curve of the aorta.
2. The secondary flow induced by the multiple planes of curvature results in a torsional flow in the aorta and such a rotational flow is observed even in the descending aorta.
3. The area at inner curve of the bend during acceleration and peak flow contains longer vortical structure that might contribute to higher blood clot potential.

#### References

- [1] Zakaria, Mohamad Shukri, Farzad Ismail, Masaaki Tamagawa, Ahmad Fazli Abdul Aziz, Surjatin Wiriadidjaja, Adi Azrif Basri, and Kamarul Arifin Ahmad. "Review of numerical methods for simulation of mechanical heart valves and the potential for blood clotting." *Medical & biological engineering & computing* 55, no. 9 (2017): 1519-1548.
- [2] Yin, Wei, Yared Alemu, Klaus Affeld, Jolyon Jesty, and Danny Bluestein. "Flow-induced platelet activation in bileaflet and monoleaflet mechanical heart valves." *Annals of biomedical engineering* 32, no. 8 (2004): 1058-1066.
- [3] Basri, Adi A., Mohamed Zubair, Ahmad FA Aziz, Rosli M. Ali, Masaaki Tamagawa, and Kamarul A. Ahmad. "Computational fluid dynamics study of the aortic valve opening on hemodynamics characteristics." In *Biomedical Engineering and Sciences (IECBES), 2014 IEEE Conference on*, pp. 99-102. IEEE, 2014.
- [4] Zakaria, M. S., F. Ismail, S. Wiriadidjaja, M. F. A. Aziz, M. Tamagawa, A. A. Basri, and K. A. Ahmad. "Numerical simulation of mechanical heart valve with coherent vortex shedding in OpenFOAM." *Proceedings of Mechanical Engineering Research Day 2017* 2017 (2017): 68-69.
- [5] Biasetti, Jacopo, Fazle Hussain, and T. Christian Gasser. "Blood flow and coherent vortices in the normal and aneurysmatic aortas: a fluid dynamical approach to intra-luminal thrombus formation." *Journal of The Royal Society Interface* (2011): rsif20110041.
- [6] Jeong, Jinhee, and Fazle Hussain. "On the identification of a vortex." *Journal of fluid mechanics* 285 (1995): 69-94.

- [7] Ab Naim, Wan Naimah Wan, Poo Balan Ganesan, Zhonghua Sun, Yih Miin Liew, Yi Qian, Chang-Joon Lee, Shirley Jansen, Shahrul Amry Hashim, and Einly Lim. "Prediction of thrombus formation using vortical structures presentation in Stanford type B aortic dissection: a preliminary study using CFD approach." *Applied Mathematical Modelling* 40, no. 4 (2016): 3115-3127.
- [8] Anupindi, Kameswararao, Yann Delorme, Dinesh A. Shetty, and Steven H. Frankel. "A novel multiblock immersed boundary method for large eddy simulation of complex arterial hemodynamics." *Journal of computational physics* 254 (2013): 200-218.
- [9] Zakaria, Mohamad Shukri, Farzad Ismail, Masaaki Tamagawa, Ahmad Fazli Abdul Aziz, Surjatin Wiriadidjaja, Adi Azrif Basri, and Kamarul Arifin Ahmad. "Review of numerical methods for simulation of mechanical heart valves and the potential for blood clotting." *Medical & biological engineering & computing* 55, no. 9 (2017): 1519-1548.
- [10] Dasi, L. P., L. Ge, H. A. Simon, F. Sotiropoulos, and A. P. Yoganathan. "Vorticity dynamics of a bileaflet mechanical heart valve in an axisymmetric aorta." *Physics of Fluids* 19, no. 6 (2007): 067105.
- [11] Benim, A. C., A. Nahavandi, A. Assmann, D. Schubert, P. Feindt, and S. H. Suh. "Simulation of blood flow in human aorta with emphasis on outlet boundary conditions." *Applied Mathematical Modelling* 35, no. 7 (2011): 3175-3188.
- [12] N. H. Shaharuddin, M. A. Mohamed Sukri, S. Mansor, S. Muhamad, A. Z. S. Sheikh Salim, and M. Usman, "Flow simulations of generic vehicle model SAE type 4 and DrivAer Fastback using OpenFOAM," *J. Adv. Res. Fluid Mech. Therm. Sci.* 37, no. 1 (2017): 18–31.
- [13] Zakaria, Mohamad Shukri, Farzad Ismail, Masaaki Tamagawa, Ahmad Fazli Abdul Aziz, Surjatin Wiriadidjaya, Adi Azrif Basri, and Kamarul Arifin Ahmad. "Numerical analysis using a fixed grid method for cardiovascular flow application." *Journal of Medical Imaging and Health Informatics* 6, no. 6 (2016): 1483-1488.
- [14] L. C. Earn, T. W. Yen, and T. L. Ken, "The investigation on SIMPLE and SIMPLER algorithm through lid driven cavity," *J. Adv. Res. Fluid Mech. Therm. Sci.* 29, no. 1 (2017): 10–23.
- [15] Borazjani, Iman, Liang Ge, Trung Le, and Fotis Sotiropoulos. "A parallel overset-curvilinear-immersed boundary framework for simulating complex 3D incompressible flows." *Computers & fluids* 77 (2013): 76-96.
- [16] Ge, Liang, and Fotis Sotiropoulos. "A numerical method for solving the 3D unsteady incompressible Navier–Stokes equations in curvilinear domains with complex immersed boundaries." *Journal of computational physics* 225, no. 2 (2007): 1782-1809.
- [17] Dillard, Seth I., John A. Mousel, Liza Shrestha, Madhavan L. Raghavan, and Sarah C. Vigmostad. "From medical images to flow computations without user-generated meshes." *International journal for numerical methods in biomedical engineering* 30, no. 10 (2014): 1057-1083.
- [18] M. K. Wong, L. C. Sheng, C. S. N. Azwadi, and G. A. Hashim, "Numerical Study of Turbulent Flow in Pipe with Sudden Expansion," *J. Adv. Res. Fluid Mech. Therm. Sci.* 6, no. 1 (2015): 34–48.
- [19] Van de Vosse, F. N., A. A. Van Steenhoven, A. Segal, and J. D. Janssen. "A finite element analysis of the steady laminar entrance flow in a 90 curved tube." *International journal for numerical methods in fluids* 9, no. 3 (1989): 275-287.
- [20] Robertson, E., V. Choudhury, S. Bhushan, and D. K. Walters. "Validation of OpenFOAM numerical methods and turbulence models for incompressible bluff body flows." *Computers & Fluids* 123 (2015): 122-145.
- [21] Hunt, Julian CR, Alan A. Wray, and Parviz Moin. "Eddies, streams, and convergence zones in turbulent flows." (1988).